Progress In Electromagnetics Research C, Vol. 62, 119–129, 2016

Design of High-Isolation Compact MIMO Antenna for UWB Application

Narges Malekpour and Mohammad A. Honarvar*

Abstract—In this paper, a compact multiple-input-multiple-output (MIMO) antenna is proposed for ultra wideband (UWB) communication. The UWB MIMO antenna consists of two identical monopole antenna elements with a comb-line structure on the ground plane to improve impedance matching and enhance isolation. Simulation and measurement have been analysed in terms of reflection coefficient, mutual coupling, dispersion diagram, radiation pattern, peak gain, efficiency and envelope correlation coefficient. Results show that the antenna has an impedance bandwidth larger than 3.1–10.6 GHz, mutual coupling between the two ports lower than −25 dB and envelope correlation coefficient less than 0.001 across the UWB band. The proposed antenna has a compact size of $26 \times 31\,\text{mm}^2$. All the measured and calculated results show that the proposed UWB MIMO antenna is a good candidate for UWB MIMO systems.

1. INTRODUCTION

The Federal Communications Commission (FCC) allocated frequency band 3.1–10.6 GHz for applications with low power emission in 2002 [1]. Low power and high data rate interference immunity are the fundamental advantages of UWB communication system. However, the low transmitted power limits UWB systems to short-range communication. In order to increase data rate and/or overcome multipath fading, the multiple-input multiple-output (MIMO)/diversity technology has been considered for UWB systems. MIMO has been introduced as an efficient technique to increase channel capacity while needing no additional power or bandwidth. Both MIMO and UWB systems require high isolation among the antenna elements in the operating bands. However, by installing multiple antenna elements on the confined space, the mutual coupling between the UWB antenna elements can be very large. Thus, it is a challenge to design UWB MIMO antenna with extremely compact structures and low mutual coupling. In [2], a circular loop frequency selective surface was designed to improve the gain of the UWB antenna. In [3], a miniaturized UWB antenna was designed for WLAN and WiMax applications. WLAN and WiMax bands were achieved by using slotted ground structure and metamaterial rectangular split ring resonator. Many MIMO antennas have been proposed to reduce the mutual coupling for UWB systems [4–18]. In [4–8], various decoupling structures have been inserted between two antenna elements to enhance wide band isolation. In [9, 10], MIMO antenna has been proposed for WLAN and with a dual-band. A slotted CSRR has been inserted on the ground plane to enhance isolation. In addition, the slotted CSRR has the ability to miniaturize the antenna. In [11], antenna elements were set orthogonally with respect to each other to enhance isolation and pattern diversity. The UWB MIMO antenna reported in [12] can achieve dual reject bands and high isolation. A dual band-notched characteristic was created by using parasitic strips and slots on the radiator. In [13, 14], Electromagnetic Band-Gap (EBG) structure was used to improve the isolation by blocking surface-waves propagation. The EBG structure with no metallic vias or vertical components was formed by etching two slots and

Received 9 December 2015, Accepted 28 January 2016, Scheduled 1 March 2016
* Corresponding author: Mohammad Amin Honarvar (Amin.Honarvar@pel.iaun.ac.ir).
The authors are with the Department of Electrical Engineering, Najafabad Branch, Islamic Azad University, Najafabad, Iran.

adding two connecting bridges to a conventional uniplanar EBG unit-cell. Considering the fact that many MIMO antennas have been proposed, there are only few papers of MIMO technique in UWB systems. For those which could cover the whole UWB band [5, 6, 11, 12, 15–20], the size of the antenna in [5, 6, 11, 16, 17] is still relatively large. Recently, UWB MIMO antennas with notch-band characteristic have been introduced [21, 22]. However, in [22], the antenna had the compact size of $22 \times 36\,\text{mm}^2$, but $|S_{21}|$ was less than $-15\,\text{dB}$ for the UWB operation band.

In this paper, a compact UWB MIMO antenna is proposed. A staircase structure is formed on the radiating element to cause a wide bandwidth for UWB applications. The aim of MIMO antenna design is to reduce mutual coupling between antenna elements. A comb-line structure acting as an electromagnetic band-gap structure was used to suppress the coupling between the two elements. The size of the proposed antenna is $26 \times 31\,\text{mm}^2$, which is smaller than most of UWB antennas with a single antenna element. The simulated and measured results show a bandwidth ranging from 2.8 to 11.9 GHz.

The remaining sections of this paper are organized as follows. Section 2 represents the geometry of the proposed UWB MIMO antenna. In Section 3, the mechanism of the UWB MIMO antenna is investigated. Section 4 presents the simulation and measurement results, and finally, a conclusion is given in Section 5.

2. ANTENNA DESIGN

The prototype and geometry of the proposed compact UWB MIMO antenna is shown in Figure 1. Two antenna elements are printed on a $26 \times 31\,\text{mm}^2$ Rogers substrate, RO4003, with a thickness of 0.7874 mm and relative permittivity of 3.55. The loss tangent of the substrate is 0.0027. The UWB MIMO antenna consists of two monopole antenna elements, denoted as element 1 and element 2 in Figure 1. The radiating element is U-shaped, and there is a staircase structure which is symmetrical to the two bottom corners of the radiating element. Installing multiple antenna elements on the confined space, the mutual coupling between the UWB antenna elements can be very large. Thus, it is a challenge to design UWB MIMO antenna with extremely compact structures and low mutual coupling. The antenna elements are placed in H-plane. The edge-to-edge spacing between the elements is chosen to be 8 mm which is equivalent to $0.18\lambda_0$, and λ_0 is the free space wavelength corresponding to the centre frequency of 6.85 GHz. Each of the antenna elements is fed by a 50-Ω microstrip line. The dimensions of these microstrip lines are $Wf \times Lf\,\text{mm}^2$. The dimensions of the ground plane are $W \times Lg\,\text{mm}^2$, and a rectangular slot with dimension of $Wfs \times Lfs\,\text{mm}^2$ is cut on the top edge of the ground plane underneath each feeding line, which is used to improve the impedance matching at high frequencies. The final design stage was to add ground stubs linked by a metal strip with dimension of $Ws \times Ls\,\text{mm}^2$, which formed

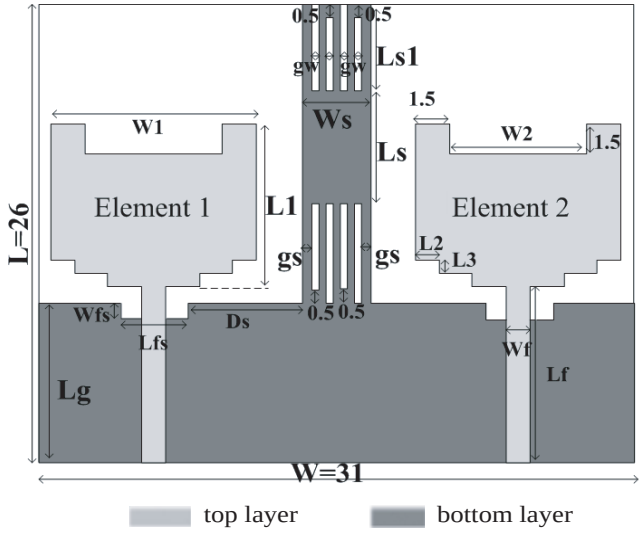

Figure 1. Geometry of the proposed antenna.

Table 1. Dimensions of the proposed antenna (mm).

L	Lfs	Lf	L_1	L_2	L_3	Lg	Ls	Ds	gs
26	4	9	8	1.5	0.5	8	7	6	0.45
W	Wfs	Wf	W_1	W_2	W_3	W_4	Ws	Ls_1	gw
31	0.8	1.4	11	8	5	8	3	5	0.3

a comb-line structure on the ground plane of the antenna. Various techniques have been investigated to combine UWB technology with MIMO techniques to reduce the mutual coupling between elements while attaining a compact size. It is shown that the proposed comb-line structure can efficiently enhance isolation and increase impedance bandwidth across the whole UWB band. The detailed parameters of the proposed antenna are provided in Figure 1. The proposed UWB MIMO antenna has been designed and analyzed by Ansys HFSS v.15. The optimized dimensions for the MIMO antenna are listed in Table 1 and used to fabricate the UWB MIMO antenna.

3. DISCUSSION OF ANTENNA DESIGN

3.1. Antenna Elements

The proposed UWB MIMO antenna consists of two identical antenna elements. The antenna element is similar to the one stated in [23], but the large size of the radiator makes the antenna in [23] unsuitable for the UWB MIMO antenna. The frequency corresponding to the lower resonances of a rectangular planar monopole antenna can be approximately calculated by [24]:

$$F_{rl} = \frac{144}{Lg + L_1 + g + \frac{w}{2\Pi\sqrt{1+\varepsilon_r}} + \frac{w_1}{2\Pi\sqrt{1+\varepsilon_r}}} \text{GHz}. \tag{1}$$

Based on Formula (1), a planar monopole antenna is designed as shown in Figure 2(a). If Lg and L_1 denote the length of the ground plane and radiation patch, respectively, and g is the gap between them, according to Eq. (1), the calculated F_{rl} (for $Lg = 8.5\,\text{mm}$, $L_1 = 10\,\text{mm}$, $g = 0.5\,\text{mm}$) is 6.8 GHz. The simulated lower resonance frequency is also about 6.8 GHz as shown in Figure 2(c), indicating good agreements between the simulated and calculated results. Figure 2(c) shows that the simulated $|S_{11}|$ is larger than $-10\,\text{dB}$ for the UWB operation, because the compact size of the antenna element and

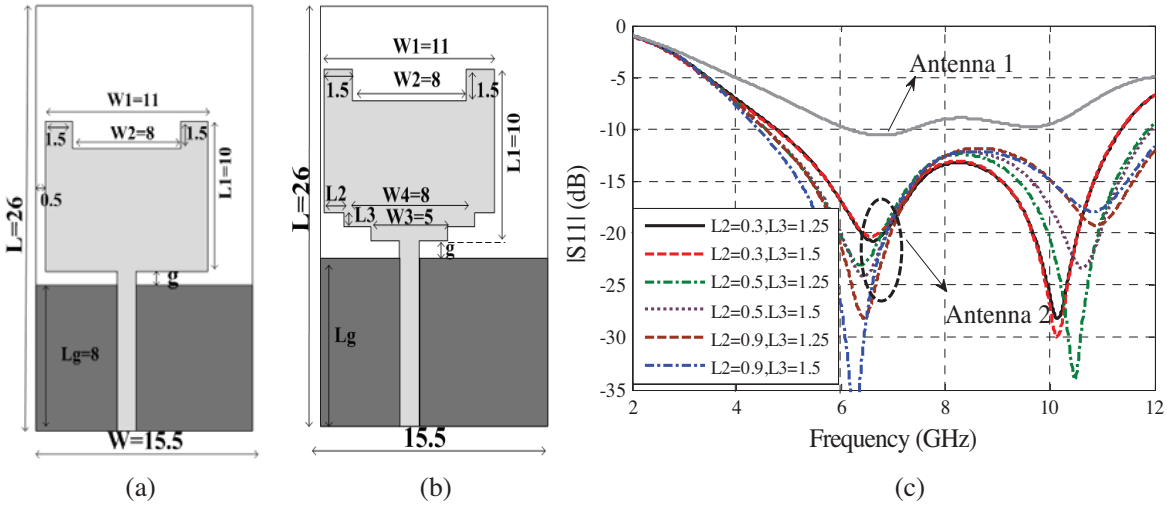

Figure 2. (a) Configuration of antenna 1, (b) configuration of antenna 2, and (c) $|S_{11}|$ of antennas 1 and 2.

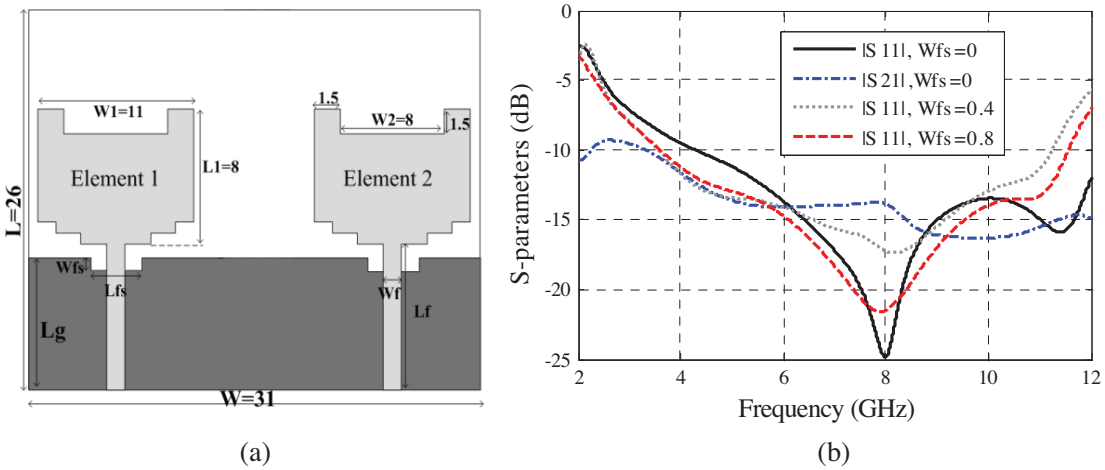

Figure 3. MIMO antenna: (a) configurations and (b) simulated S-parameters.

ground plane result in poor impedance matching. To shift the resonant frequency to lower frequency and improve input impedance matching, a staircase structure is applied by the UWB antenna presented in Figure 2(b). Moreover, by changing L_2 and L_3, the lower cut of frequency could be varied from 6 GHz to about 4.5 GHz. The variation of $|S_{11}|$ with different L_2 and L_3 implies that the staircase has great effect on the input impedance matching, as shown in Figure 2(c). Observing the $|S_{11}|$ response, a return loss of UWB antenna 2 is better than the other one. On the other hand, when the two antennas are placed close to each other as shown in Figure 3(a), the bandwidth still cannot cover the entire UWB frequency band as shown in Figure 3(b). For improving impedance matching at the low and high frequencies, a small rectangular slot in $Wfs \times Lfs\,\text{mm}^2$ is cut on the ground plane. Also by changing Wfs from 0 to 0.8 mm, the high cut of frequency varies from more than 12 GHz to about 11.2 GHz. Overall, as shown in Figure 3(b), the isolation without any decoupling structure is between 10 and 16 dB across the frequency band.

3.2. Improvement of Isolation

Mutual coupling between antenna elements should be minimized in order to maintain high efficiency of the overall system. To reduce the mutual coupling in the UWB band, a comb-line structure is applied in the proposed UWB MIMO antenna. The high isolation can be achieved with the comb-line structure, and this is mainly because of two mechanisms. One is that stubs on the ground plane, shown in Figure 4(a), can reduce the mutual coupling between the two antenna elements by capturing the current toward them, except the frequency band of 5–6 GHz. The simulated S_{11} and S_{21} of the MIMO antenna are shown in Figure 4(b). Note that due to the symmetrical structure of the antenna and as S_{22} and S_{12} are identical to S_{11} and S_{21}, respectively, we have only marked S_{11} and S_{21} in Figures 4(b) and (c). Using stubs increased the isolation between the two radiators, which improved the impedance matching that satisfied the requirements for UWB operation, compared with the case without any decoupling structure.

The other mechanism is that stubs on the ground plane are linked by a small metal strip with dimension of $Ws \times Ls\,\text{mm}^2$, in order to reduce the mutual coupling for the band of 5–6 GHz and to act as an EBG structure, as shown in Figure 5(a). This has formed a comb-line structure on the ground plane of the antenna. The proposed comb-line structure improves the mutual coupling for the band of 5–6 GHz, and the isolation is larger than -25 dB for the frequency band of 3.1–10.6 GHz, shown in Figure 5(b). The variation of $|S_{21}|$ with different Ws implies that the metal strip has a great effect on the mutual coupling.

The proposed EBG structure is shown in Figures 6(a) and (b). An EBG structure can be described by an equivalent capacitance C, introduced by the gaps between the adjacent stubs, and furthermore, inductor L is the result of the current flowing through the stubs. The center frequency of the bandgap

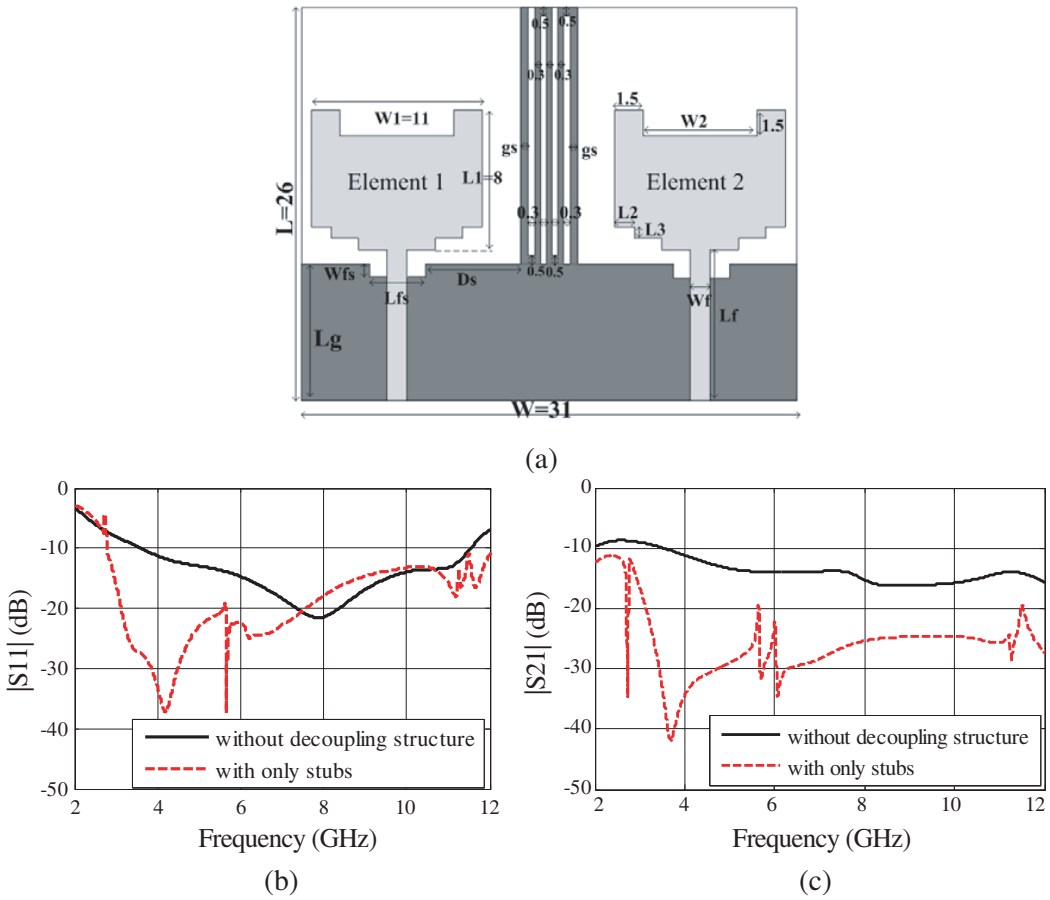

Figure 4. (a) Geometries of MIMO antenna, (b) and (c) simulated S-parameters.

is given by [25]:

$$f_c = \frac{1}{2\pi\sqrt{lc}}\,\text{GHz}. \tag{2}$$

In order to predict the frequency selective behavior of the EBG structures, the dispersion characteristics should be extracted. The dispersion characteristic is the plot of propagation constant of every mode versus frequency. To obtain such plots, eigenvalues of the electromagnetic problem should be found. Band gaps occur in frequency intervals, where no dispersion curves in the slow-wave region are present. To show the effectiveness of the band-gap design, the dispersion diagram of the optimized dimension EBG structure is plotted in Figure 6(c) based on the eigenmode analysis. Finally, EBG cell dimensions are tuned to have a bandgap over the desired frequency band.

To further investigate the effect of the comb-line structure, the simulated current distributions of the antenna with and without a comb-line structure at 6.5 and 9 GHz are shown in Figure 7. Without using the comb-line structure, when port 1 is exited and port 2 terminated with a 50-Ω load, a strong induced current appears on port 2. Moreover, a certain amount of ground current also flows to the ground plane of the other element when the two antennas are closely placed. The obtained current increases mutual coupling between the two ports. However, when the comb-line structure is added on the ground plane and port 1 exited, significant amounts of current are coupled on the comb-line structure, which weakens the induced current on port 2 of the antenna element. Thereby, a low mutual coupling between the two ports is achieved. This effect is the same when port 2 is exited and port 1 terminated with a 50-Ω load.

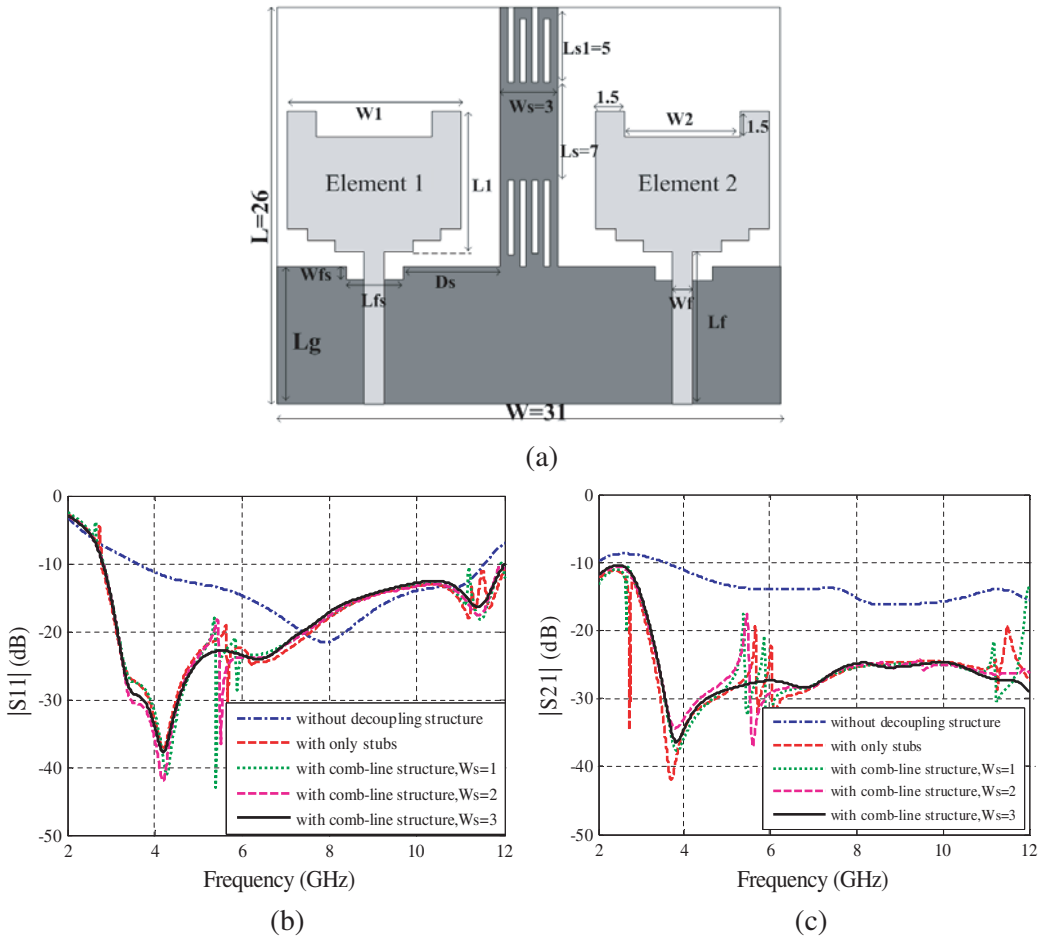

Figure 5. (a) Geometries of MIMO antenna with EBG structure, (b) and (c) simulated S-parameters.

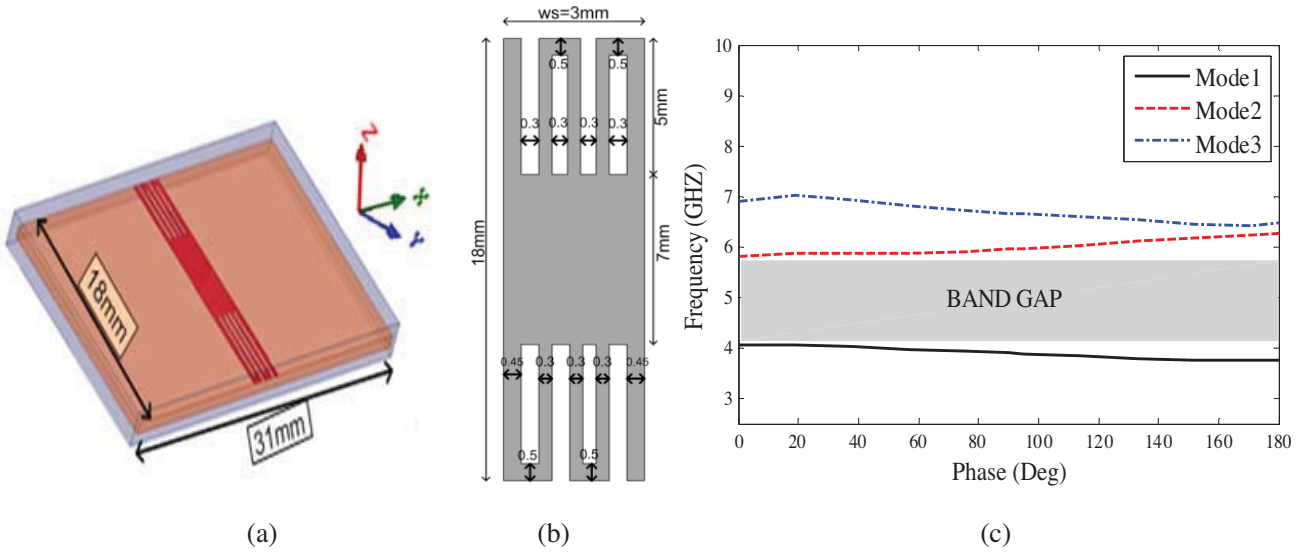

Figure 6. (a) 3-D view of the EBG cell, (b) cell of the EBG structure with dimensions, (c) dispersion diagram of the proposed EBG using three mode eigenmode solver.

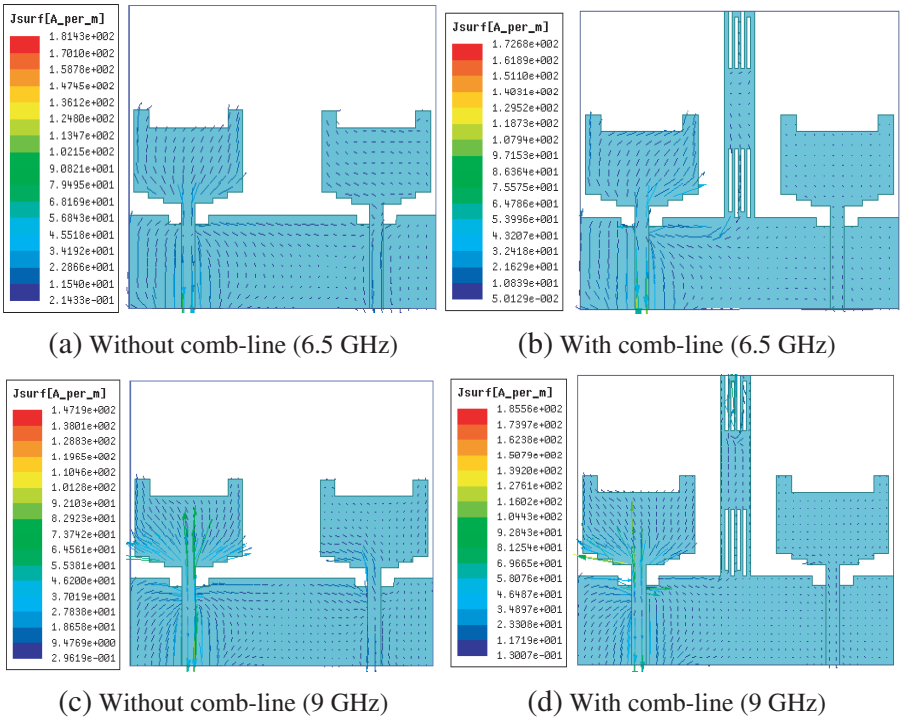

(a) Without comb-line (6.5 GHz) (b) With comb-line (6.5 GHz)

(c) Without comb-line (9 GHz) (d) With comb-line (9 GHz)

Figure 7. Current distribution of the UWB MIMO antenna with and without comb-line structure.

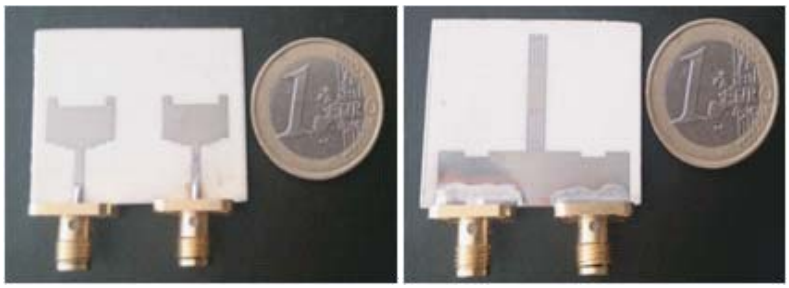

Figure 8. Photographs of the fabricated antenna.

4. RESULTS AND DISCUSSIONS

A prototype of the MIMO antenna described in Section 2 has been fabricated and tested. Photos of the fabricated UWB MIMO antenna are presented in Figure 8, and the simulated and measured s-parameters of the final design are in good agreement as shown in Figure 9. The impedance bandwidth ($S_{11} < -10$ dB) can cover the whole UWB 3.1–10.6 GHz and the mutual coupling less than -25 dB cover the UWB band. Any discrepancy is attributed to manufacturing tolerance and non-precise SMA connection. These results prove that this antenna is a good candidate for MIMO operation across the UWB band.

4.1. Radiation Patterns

The measured radiation patterns of the proposed MIMO antenna at the frequencies of 3 GHz, 6 GHz and 10 GHz in the x-z (H) and y-z (E) planes when port 1 is excited and port 2 terminated with a 50-Ω load are shown in Figures 10(a), (b) and (c), respectively. Note that, in Figure 11, the radiation patterns in the H-plane are quasi-omnidirectional to receive the signals from all directions.

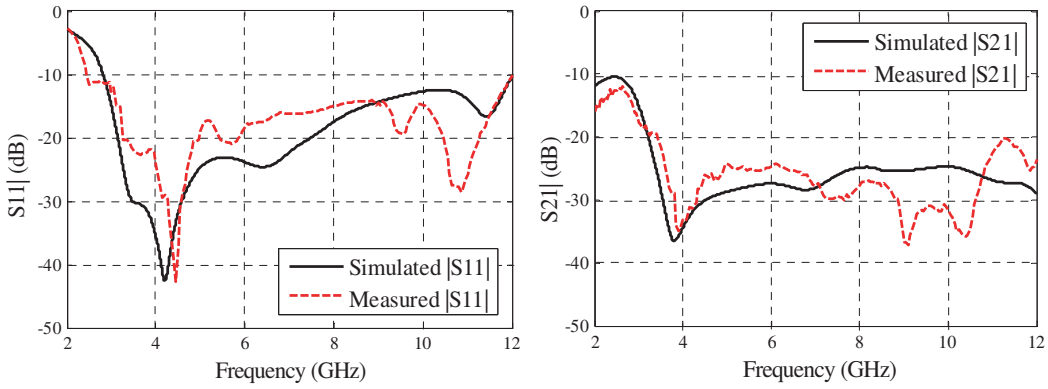

Figure 9. The measured and simulated *s*-parameters of the proposed antenna.

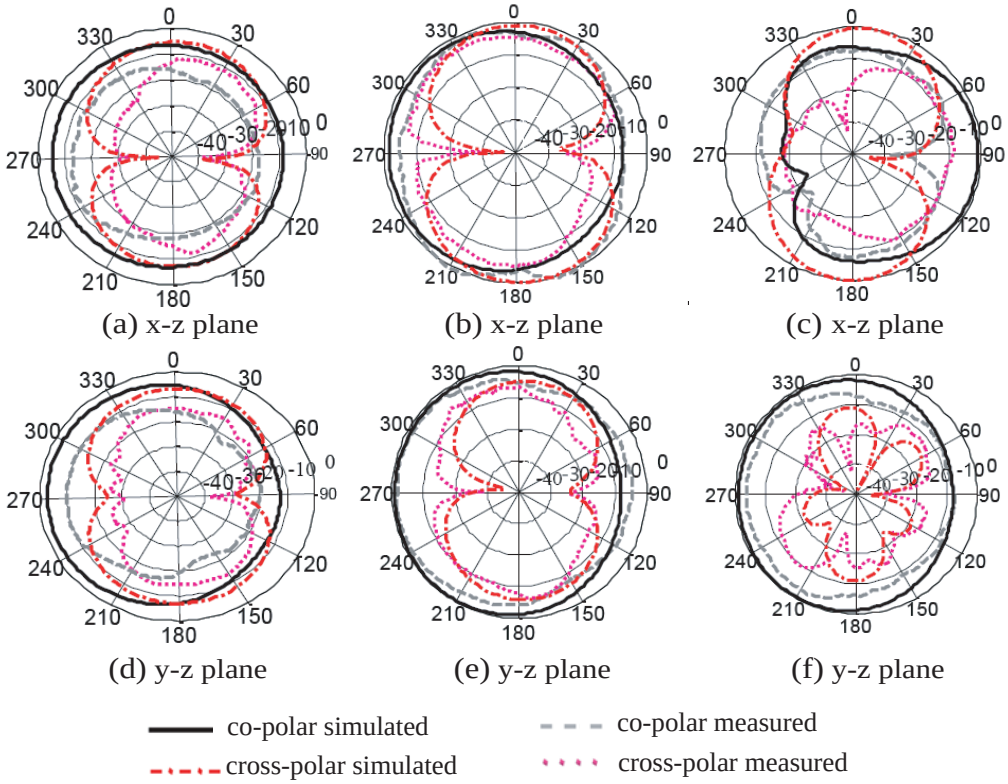

Figure 10. Measured radiation patterns with port 1 excited and port 2 terminated with 50-Ω load: (a) (d) at 3 GHz, and (b) (e) at 6 GHz, and (c) (f) at 10 GHz.

The simulated and measured gains of the antenna are shown in Figure 11(a). Only the gain for port 1 is presented, and during the measurements, only port 1 is excited, while port 2 is terminated with a 50-Ω load. The measured gain ranges from −2 to 5.8 dBi across the UWB band. The simulated and measured efficiencies of the antenna shown Figure 11(b) indicate that the discrepancies of the simulated and measured efficiencies are small, and the measured efficiency is above 95% across the frequency band.

4.2. Envelope Correlation Coefficient

Envelope correlation coefficient (ECC) is an important parameter for evaluating the MIMO/diversity performance. Two methods can be used to find ECC: 1) based on the far-field radiation pattern;

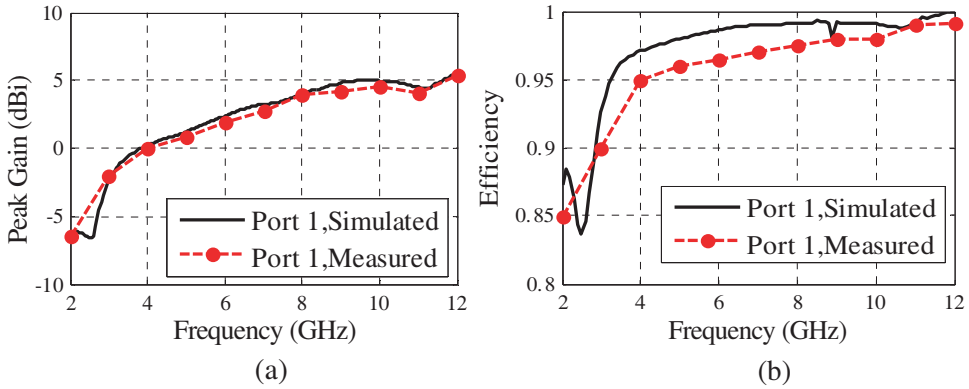

Figure 11. (a) Peak gain and (b) efficiency of MIMO antenna.

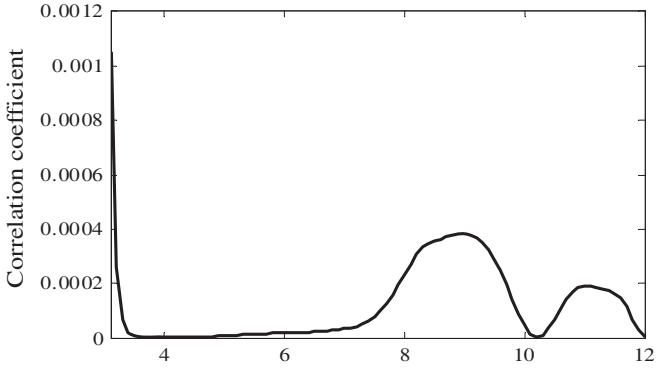

Figure 12. Correlation coefficient for the MIMO antenna.

2) based on the knowledge of scattering parameters. The far-field method is very time-consuming and requires complex and advanced calculations. Therefore, s-parameter method is adopted for the calculated correlation coefficient in this study, as in [26, 27]:

$$\rho_e = \frac{|s_{12}s_{11}^* + s_{22}s_{21}^*|^2}{[1-(|s_{11}|^2+|s_{21}|^2)][1-(|s_{22}|^2+|S_{12}|^2)]}. \tag{3}$$

The calculated result of the proposed MIMO antenna is exhibited in Figure 12. It shows that the proposed antenna has the ECC less than 0.001. Since the obtained ECC value is close to zero, the proposed antenna is more suitable for MIMO communications.

Table 2. Performance comparisons of the proposed and reference antennas.

Reference	Size (mm^3)	Bandwidth GHz	Isolation (dB)	Band-Notched	ε_r	ρ_e	Gain (dBi)
[6]	$35 \times 40 \times 0.8$	3–11.6	-16	-	3.5	0.01	< 6.5
[11]	$26 \times 40 \times 0.8$	2.9–10.6	-15	-	3.5	0.2	< 6.5
[12]	$27 \times 30 \times 0.8$	3–11	-20	3.3–3.7; 5.1–5.8	4.4	0.012	< 5.25
[16]	$32 \times 32 \times 0.8$	3.1–10.6	-15	-	4.4	0.04	< 4.2
[22]	$22 \times 36 \times 1.6$	3.1–11	-15	5.1–5.8	3.5	0.1	< 4.5
This work	$26 \times 31 \times 0.78$	2.8–12	-25	-	3.35	0.001	< 5

4.3. Performance Comparison

Comparisons of the proposed antenna and recently reported UWB MIMO antennas [6, 11, 12, 16, 22] on the bandwidth, envelope correlation coefficient, size and isolation are listed in Table 2. The proposed UWB MIMO antenna achieves significant reduction in ECC, which means that the proposed antenna has a good isolation performance. Besides, other characteristics such as type of substrate and isolation are studied as well. Therefore, the results show that the proposed antenna with compact size and high isolation is a good candidate for MIMO system applications.

5. CONCLUSION

By using a comb-line structure, a compact UWB MIMO antenna with improved isolation for a UWB application is proposed in this paper. The simulated and measured results have shown that the antenna can cover the UWB band of 3.1–10.6 GHz with better isolation than −25 dB in the whole UWB. The radiation patterns, gain and efficiency have also been measured. Measured results have shown that the MIMO antenna can achieve an envelope correlation coefficient of less than 0.001 across the UWB. Based on the measured and simulated antenna performances, we are convinced that the MIMO antenna is a good candidate for portable UWB applications.

REFERENCES

1. Federal Communications Commission, "Revision of Part 15 of the commission's rules regarding ultra-wideband transmission system," 98–153, First Report and Order, ET Docket, FCC, Washington, D.C., 2002.
2. Saraswat, R. K. and M. Kumar, "A frequency band reconfigurable UWB antenna for high gain applications," *Progress In Electromagnetics Research B*, Vol. 64, 29–45, 2015.
3. Saraswat, R. K. and M. Kumar, "Miniaturized slotted ground UWB antenna loaded with metamaterial for WLAN and WiMAX applications," *Progress In Electromagnetics Research B*, Vol. 65, 65–80, 2016.
4. Singh, H. S., B. R. Meruva, G. K. Pandey, P. K. Bharti, and M. K. Meshram, "Low mutual coupling between MIMO antennas by using two folded shorting strips," *Progress In Electromagnetics Research B*, Vol. 53, 205–221, 2013.
5. Bilal, M., R. Saleem, M. F. Shafique, and H. A. Khan, "MIMO application UWB antenna doublet incorporating a sinusoidal decoupling structure," *Microw. Opt. Technol. Lett.*, Vol. 56, 1547–1553, 2014.
6. Zhang, S., Z. Ying, J. Xiong, and S. He, "Ultrawideband MIMO/diversity antennas with a tree-like structure to enhance wideband isolation," *IEEE Antennas Wireless Propag. Lett.*, Vol. 8, 1279–1282, 2009.
7. Arun, H., A. K. Sarma, M. Kanagasabai, S. Velan, C. Raviteja, and M. G. N. Alsath, "Deployment of modified serpentine structure for mutual coupling reduction in MIMO antennas," *IEEE Antennas Wireless Propag. Lett.*, Vol. 13, 277–280, 2014.
8. Sharawi, M. S., A. B. Numan, and D. N. Aloi, "Isolation improvement in a dual-band dual-element MIMO antenna system using capacitively loaded loops," *Progress In Electromagnetics Research*, Vol. 134, 247–266, 2013.
9. Yang, D.-G., D. O. Kim, and C.-Y. Kim, "Design of dual-band MIMO monopole antenna with high isolation using slotted CSSRR for WLAN," *Microw. Opt. Technol. Lett.*, Vol. 56, 2252–2257, 2014.
10. Zhai, H., Z. Ma, and C. Liang, "Reduction of dual-band mutual couplings between two antennas by dual-band single-negative epsilon metamaterials," *Journal of Electromagnetic Waves and Applications*, Vol. 28, No. 3, 281–288, 2013.
11. Liu, L., S. W. Cheung, and T. I. Yuk, "Compact MIMO antenna for portable devices in UWB applications," *IEEE Trans. Antennas Propag.*, Vol. 61, 4257–4264, 2013.
12. Li, J. F., Q. X. Chu, Z. H. Li, and X. Xia, "Compact dual band-notched UWB MIMO antenna with high isolation," *IEEE Trans. Antennas Propag.*, Vol. 61, 4759–4766, 2013.

13. Al-Hasan, M. J., T. A. Denidni, and A. R. Sebak, "Millimeter-wave compact EBG structure for mutual coupling reduction applications," *IEEE Trans. Antennas Propag.*, Vol. 6, 823–828, 2014.
14. Zhang, X.-Y., X. Zhong, B. Li, and Y. Yu, "A dual-polarized MIMO antenna with EBG for 5.8 GHz WLAN application," *Progress In Electromagnetics Research Letters*, Vol. 51, 15–20, 2015.
15. Liu, L., Z. D. Wang, Y. Z. Yin, J. Ren, and J. J. Wu, "A compact ultrawideband MIMO antenna using QSCA foe high isolation," *IEEE Antennas Wireless Propag. Lett.*, Vol. 13, 1497–1500, 2014.
16. Ren, J., W. Hu, Y. Yin, and R. Fan, "Compact printed MIMO antenna for UWB applications," *IEEE Antennas Wireless Propag. Lett.*, Vol. 13, 1517–1520, 2014.
17. Liu, Y. F., P. Wang, and H. Qin, "Compact ACS-fed UWB antenna for diversity applications," *IET Electron. Lett.*, Vol. 50, 1336–1338, 2014.
18. Khan, M. S., A. D. Capobianco, A. I. Najam, I. Shoaib, E. Autizi, and M. F. Shafique, "Compact ultra-wideband diversity antenna with a floating parasitic digitated decoupling structure," *IET Microwaves Antenna and Propag.*, Vol. 8, 747–753, 2014.
19. Mao, C. X. and Q. X. Chu, "Compact coradiator UWB-MIMO antenna with dual polarization," *IEEE Trans. Antennas Propag.*, Vol. 62, 4474–4479, 2014.
20. Khan, M. S., A.-D. Capobianco, A. Iftikhar, S. Asif, and B. D. Braaten, "A compact dual polarized ultrawideband multiple-input multiple-output antenna," *Microw. Opt. Technol. Lett.*, Vol. 58, 163–166, 2016.
21. Khan, M. S., A. D. Capobianco, S. Asif, A. Iftikhar, B. Ijaz, and B. D. Braaten, "Compact 4×4 UWB-MIMO antenna with WLAN band rejected operation," *Electron Lett.*, Vol. 51, 1048–1050, 2015.
22. Liu, L., S. W. Cheung, and T. I. Yuk, "Compact MIMO antenna for portable UWB applications with band-notched characteristic," *IEEE Trans. Antennas Propag.*, Vol. 63, 1917–1924, 2015.
23. Panda, J. R., A. S. R. Saladi, and R. S. Kshetrimayum, "A compact 3.4/5.5 GHz dual band-notched UWB monopole antenna with nested U-shaped slots," *Computing Communication and Networking Technologies (ICCCNT)*, 1–6, 2010.
24. Thomas, K. G. and M. Sreenivasan, "A simple ultrawideband planar rectangular printed antenna with band dispensation," *IEEE Trans. Antennas Propag.*, Vol. 58, 27–34, 2010.
25. Sievenpiper, D., L. Zhang, R. F. J. Broas, N. G. Alexopolous, and E. Yablonovitch, "High-impedance electromagnetic surfaces with a forbidden frequency band," *IEEE Trans. Microwave Theory and Techniques*, Vol. 47, 2059–2074, 1999.
26. Blanch, S., J. Romeu, and I. Corbella, "Exact representation of antenna system diversity performance from input parameter description," *Electron Lett.*, Vol. 39, 705–707, 2003.
27. Dietrich, C. B., K. Dietze, R. J. Nealy, and W. L. Stutzman, "Spatial polarization and pattern diversity for wireless handheld terminals," *IEEE Trans. Antennas Propag.*, Vol. 49, 1271–1281, 2001.